ISIJ International, Vol. 56 (2016), No. 7, pp. 1226–1231

Friction Lap Joining of Thermoplastic Materials to Carbon Steel

Kimiaki NAGATSUKA,[1)]* Daiki KITAGAWA,[1)] Hiroto YAMAOKA[2)] and Kazuhiro NAKATA[1)]

1) Joining and Welding Research Institute, Osaka University, 11-1, Mihogaoka, Ibaraki, Osaka, 567-0047 Japan.
2) IHI Corporation, 1, Shin-nakahara-cho, Isogo-ku, Yokohama, 235-8501 Japan.

(*Received on January 25, 2016; accepted on March 25, 2016; J-STAGE Advance published date: May 24, 2016*)

Dissimilar material joining of polyamide 6 and polyethylene plates to a plain carbon steel (SPCC) plate was performed using friction lap joining. The polyamide 6 and SPCC plates could be directly joined by friction lap joining, whereas the polyethylene and SPCC plates could not. Corona discharge treatment of the polyethylene surface enabled the joint formation with SPCC. The tensile shear fracture load of the SPCC/polyamide 6 and SPCC/corona-discharge-treated polyethylene joints increased with the joining speed up to 600 mm min^{-1}, beyond which it decreased. These joints were fractured at the base material of the plastic plate at optimal joining speeds in the tensile shear test. Continuously joined interfaces of these materials were observed via cross-sectional microstructure analysis. Transmission electron microscopy and selected area diffraction patterns indicated that these materials were joined through the surface oxide layer of SPCC composed of Fe_3O_4. The relation between the tensile shear fracture loads and the results of XPS analysis indicated that polar groups such as amide, hydroxyl, and carboxyl groups on the plastic surfaces were highly effective for joint formation of the SPCC/plastic joints.

KEY WORDS: friction lap joining; plain carbon steel; polyamide 6; polyethylene; corona discharge treatment; polar group; dissimilar material joining.

1. Introduction

Dissimilar material joining techniques have been developed to join lightweight materials to conventional construction materials in order to reduce the weight of vehicles. For instance, a multi-material structure of steel and an Al alloy joined by friction stir welding (FSW) has been in practical use in the automobile industry.[1)] Plastics and their composites, such as carbon-fiber-reinforced plastics (CFRPs), have attracted considerable attention in the automobile and aircraft industries as novel construction materials for attaining significant weight reduction. In particular, thermoplastic materials, such as polyamide (PA), polyethylene (PE), polypropylene (PP), and polyphenylene sulfide (PPS), and carbon-fiber-reinforced thermoplastics (CFRTPs), which are composites of a thermoplastic matrix and carbon fibers, not only exhibit high specific strength and toughness but also are highly processable because they can be formed via press forming and injection molding.[2–4)] The use of such materials has sharply increased in the above-mentioned fields. Metallic materials such as carbon steel have been widely used in engineering structures and components because of their high strength and relatively low cost. To further exploit these advantages, techniques for joining dissimilar materials such as plastics and carbon steel have been demanded in order to employ plastics in a wide range of applications and improve their manufacturing production performance.

Adhesive bonding and mechanical fastening have been adopted as conventional methods for dissimilar material joining involving such materials.[5,6)] However, these methods suffer from several drawbacks. Adhesive bonding not only involves a long processing time for achieving an effective bonding force but also causes environmental pollution because of the emission of volatile organic compounds (VOCs). Mechanical fastening results in increased weight, stress concentration, and low airtightness; moreover, it is not suitable for mass production. Such problems could potentially be solved by direct joining via thermal fusion bonding. In recent years, researchers have investigated techniques for fusion bonding of dissimilar materials using various heat sources, such as laser joining,[7–9)] ultrasonic welding,[10)] induction heating,[11)] friction spot joining,[12,13)] friction stir welding,[14,15)] and friction lap joining (FLJ).[16–24)]

FLJ, which is a novel direct joining method, is derived from a FSW process. The tool used in FSW consists of a stirring probe, to facilitate material flow, and a shoulder part; however, the tool used in FLJ does not require such a probe.[1)] FLJ uses only the heat energy generated by the friction between the shoulder of the rotating tool and a metal surface; thus, the damage to the rotating tool during FLJ is less than that during FSW. In FLJ, the rotating tool is seldom deformed and consumed, even if high-melting-point metals such as steels are joined. A reusable rotating tool is pressed onto the surface of the metal and it moves along the overlap region. The plastic near the interface is heated by the heat energy transferred from the friction-heated metal, and a narrow molten region is formed on the plastic mate-

* Corresponding author: E-mail: nagatuka@jwri.osaka-u.ac.jp
DOI: http://dx.doi.org/10.2355/isijinternational.ISIJINT-2016-042

rial. Joining of the metal and the plastic is complete once the molten plastic solidifies under the tool pressure. Thus, the rotating tool not only heats the materials to be joined but also pressurizes the joint interface.[22,23] Based on these features, FLJ has the potential to achieve strong interface bonding without high-cost apparatus, strict design limitations of the joint geometry, or excessive deterioration of the base materials. Furthermore, FLJ is an energy-saving and environmental-friendly process, and it is easily controllable because it involves only a few joining parameters, such as tool dimension, rotation speed, plunge depth, and joining speed. Therefore, this technique can expand the applications of plastic materials, including CFRTPs, combined with metals.

Previous studies[17–21] on FLJ have investigated dissimilar material joining of thermoplastics (*e.g.*, polar plastics such as PA6 and ethylene acrylic acid copolymer (EAA) and non-polar plastics such as PE) to lightweight metals such as Al and Mg alloys. The possibility of directly joining polar plastics to such metals has been shown. However, only a few studies have reported dissimilar material joining techniques for steel/plastic, and the joining mechanism of these materials by FLJ has not been clarified.[16]

It is well known that FSW for steel is difficult, as the thermal strength of steel is considerably greater than that of lightweight metals. In addition to the thermal strength, the rigidity, thermal expansion coefficient, thermal conductivity, and friction coefficient of steel also differ from those of lightweight metals. Therefore, joint formation of steel/plastic by FLJ is expected to be difficult, and suitable FLJ conditions for steel/plastic would differ significantly from those for lightweight metals.

The objectives of this research are to confirm the possibility of directly joining plastic and steel, to investigate the effects of the joining speed during FLJ and of the surface modification on PE (non-polar plastic), and to clarify the direct joining mechanism of these materials. Therefore, FLJ of PA6, as-received PE, and corona-discharge-treated PE to plain carbon steel (SPCC) is performed using a position-controlled FSW machine, and the joint characteristics are investigated. Corona discharge treatment contributes to the formation of polar groups, such as hydroxyl (C–OH) and carboxyl (O=C–OH) groups, on plastic surfaces by O radical and O_3, which are generated by discharge in atmospheric air.[20]

2. Materials and Methods

Experiments were performed using polyamide 6 (PA6: $[NH(CH_2)_5CO]_n$) and polyethylene (PE: $[CH_2CH_2]_n$) plates (150 mm × 75 mm × 3 mm) as thermoplastic materials, and a plain carbon steel (SPCC) plate (150 mm × 75 mm × 2 mm). Corona discharge treatment was applied to the surface of the PE plate for 1 and 5 min in order to modify the surface condition. The surface chemical condition of as-received PA6 and as-received PE subjected to corona discharge treatment for 5 min was analyzed via X-ray photoelectron spectroscopy (XPS, Quantera SXM, Physical Electronics, Inc., Chanhassen, MN, USA). **Figure 1** shows a schematic illustration of FLJ of the plastic and metal plates. The SPCC plate was placed on the PA6 and PE plates. The PE plate was placed such that its corona-discharge-treated surface faced the SPCC plate. FLJ was used to join the SPCC plate to the plastic plates using a rotating tool made of WC–Co alloy. The tool had a shoulder of diameter 15 mm (without stirring probe) and was tilted at an angle of 3° forward from the vertical. The tool plunge depth was 0.9 mm and the tool rotation speed was 1 000 rpm, as determined by preliminary experiments. Different joining speeds in the range of 200–1 000 mm min^{-1} were employed. The temperature during FLJ was monitored using a K-type thermocouple inserted at the SPCC plate/plastic plate interface at the center of the joining line.

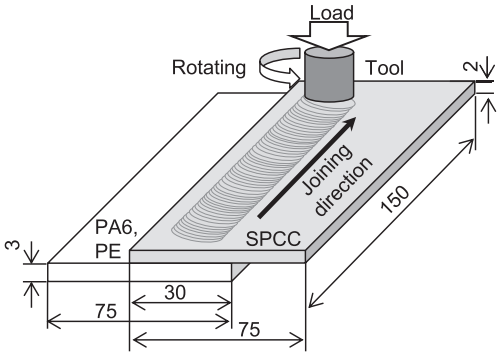

Fig. 1. Schematic illustration of friction lap joining of plastic and metal (all dimensions in mm).

The FLJ joints were cross-sectioned and mounted in epoxy resin before they were ground with #220 SiC paper and polished with diamond paste. Then, the macrostructure and microstructure of the joined interface were observed via optical microscopy (OM) and transmission electron microscopy (TEM, 2100F, JEOL, Ltd., Tokyo, Japan). Gel permeation chromatography (GPC) analysis of the PA6 plate was carried out to evaluate the changes in the molecular weight of the plastic by sampling the PA6 contacted with the interface of the FLJ joint at various joining speeds. A differential refractometer detector (Shodex RI104, Showa Denko K. K., Tokyo, Japan) was employed for the GPC analysis; the column (Shodex HFIP-606M, Showa Denko K. K., Tokyo, Japan) was maintained at a temperature of 313 K, and hexafluoroisopropyl alcohol with 5 mol m^{-3} of trifluoroacetic acid sodium salt at a flow rate of 200 mm^3 min^{-1} was used as the solvent. The molecular weight was determined relative to that of the polymethyl methacrylate standard. To evaluate the joint strength, the FLJ joints were cut into 15-mm-wide strips perpendicular to the joining direction. Tensile shear tests were carried out using a precision universal tester at a crosshead speed of 0.5 mm min^{-1}. Three strips were tested for each joining condition. The fracture surfaces of the tensile shear specimens were observed via OM.

3. Results

3.1. Effect of Polar Groups on Thermoplastic Surface on FLJ Joint Characteristics

Figure 2 shows the appearance of the FLJ joint of SPCC/PA6 at a joining speed of 600 mm min^{-1}. The tool-passed zone on the SPCC plate exhibits a smooth surface. Large weld flash was not observed in the tool-passed zone on the SPCC plate. As-received PA6 was directly joined to SPCC

without any surface treatment. In contrast, as-received PE could not be joined to SPCC. Corona discharge treatment of PE facilitated the joint formation of PE and SPCC.

Figure 3 shows the TEM bright field image (BFI) of the joined interface of SPCC/PA6 at a joining speed of 600 mm min^{-1}. The interfacial layer was observed, and Fe_3O_4 was detected by selected area diffraction (SAD) analysis of this layer. SPCC and PA6 were joined through the oxide layer of SPCC. A reaction layer, which is often formed during dissimilar material joining of metal/metal and ceramic/metal, was not observed at the interface of SPCC and PA6.

Figure 4(a) shows the tensile shear fracture load of the FLJ joints of SPCC/PA6, as-received PE, and corona-discharge-treated PE processed at a joining speed of 600 mm min^{-1}. Figures 4(b) and 4(c) show the appearances of the joints fractured at the plastic base plate and the joint interface, respectively. The SPCC/PA6 joints exhibited an average fracture load of 1.72 kN, and all the fractures occurred at the PA6 base plate. The corona discharge treatment facilitated the joining of PE to SPCC. The joint tensile shear fracture load increased with the corona discharge treatment time up to 5 min, and it attained a maximum value of around 0.95 kN owing to the PE base plate fracture.

Table 1 lists the chemical compositions measured by the wide spectra of XPS analysis of the surfaces of PA6, as-received PE, and corona-discharged-treated PE before the joining experiments. These results do not include the composition of H, because the XPS analysis could not detect the H spectrum. C was detected as the major element in every plastic. N and O were also detected from PA6 owing to the amide group (CONH). From the as-received PE, no other element was detected. O was highly detected on the corona-discharge-treated PE surface. **Figure 5** shows the C1s narrow spectra of XPS analysis of the surfaces of PA6, as-received PE, and corona-discharge-treated PE. C–C and C–H bonding were mainly detected from every plastic. Amide (O=C–NH) bonding was also detected from the PA6 surface. In addition, hydroxyl (C–OH) and carboxyl (O=C–OH) bonding were detected from the corona-discharge-treated PE but not from the as-received PE. This indicated that the hydroxyl (-OH) and carboxyl (-COOH) groups were generated by the corona discharge treatment. The plastic surface was oxidized by the O radical and O_3, which were generated by corona discharge in the air.

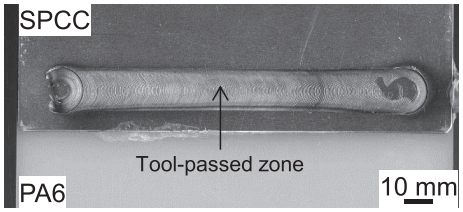

Fig. 2. Appearance of the FLJ joint of SPCC/PA6 at a joining speed of 600 mm min^{-1}.

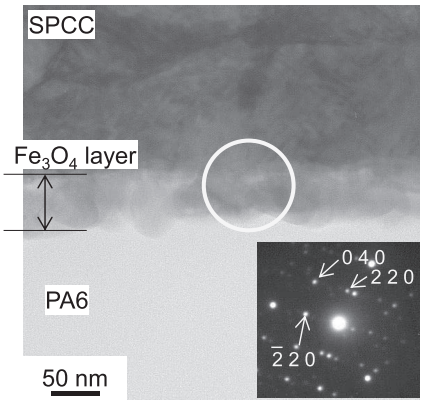

Fig. 3. TEM bright field image (BFI) of the joined interface of SPCC/PA6 at a joining speed of 600 mm min^{-1} and selected area diffraction pattern at the interface layer.

Table 1. Chemical compositions measured by the wide spectra of XPS analysis of the surfaces of PA6, as-received PE, and corona-discharged-treated PE before the joining experiments.

Specimen	C	O	N
PA6	73.3	16.4	10.3
PE (As-received)	96.3	1.4	2.3
PE (Corona-discharge treated for 5 min.)	65.0	33.8	1.2

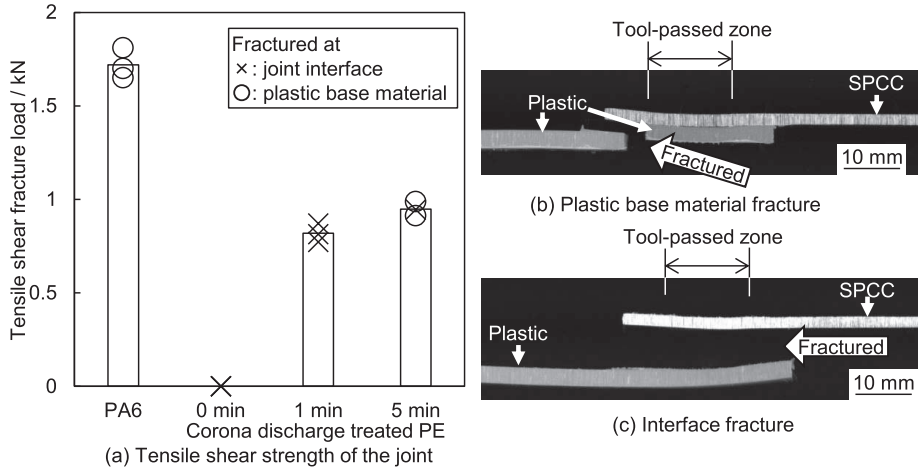

Fig. 4. (a) Tensile shear fracture load of FLJ joints of SPCC/PA6, as-received PE, and corona-discharge-treated PE processed at a joining speed of 600 mm min^{-1}, and appearances of the joints fractured at (b) the plastic base plate and (c) the joint interface.

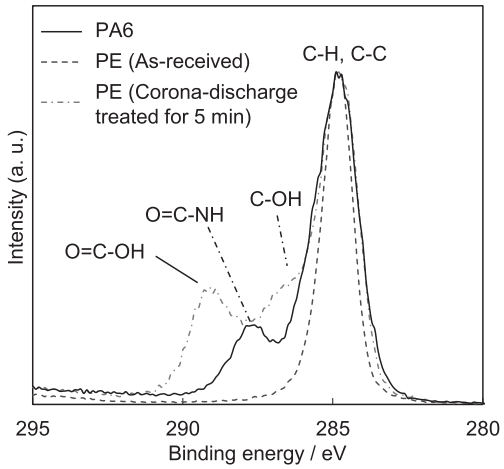

Fig. 5. C1s narrow spectra of XPS analysis of the surfaces of PA6, as-received PE, and corona-discharge-treated PE.

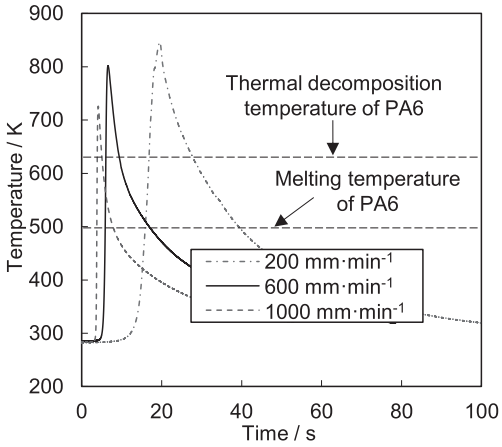

Fig. 6. Temperature history during FLJ of SPCC/PA6 at joining speeds of 200, 600, and 1 000 mm min^{-1}.

3.2. Effect of Joining Speed on FLJ Joint Characteristics

Figure 6 shows the temperature history during FLJ of SPCC/PA6 at joining speeds of 200, 600, and 1 000 mm min^{-1}. As the rotating tool approached the measured position, the temperature rapidly increased. At every joining speed, the maximum temperature during FLJ was higher than the melting temperature (approximately 498 K) and the thermal decomposition temperature (approximately 623 K) of PA6. As the joining speed decreased, the maximum temperature increased, and the melting and thermal decomposition durations (the period of time over which the temperature of PA6 exceeded these temperatures) became longer owing to the heat input increase.

Figure 7 shows the cross-sectional macrostructure of the FLJ joint of SPCC/PA6 at joining speeds of 200, 600, and 1 000 mm min^{-1}. Continuously joined interfaces of SPCC/PA6 were obtained at every joining speed. Concave-downward deformation of the SPCC plate was observed in the tool-passed zone, and this deformation increased with decreasing joining speed. Thus, the thickness of the PA6 plate also decreased, and the width and depth of the melted area in the PA6 plate increased. Voids were observed in the melted area of the PA6 plate at a joining speed of 200 mm min^{-1}. Volatile products such as H_2O and CO_2 are generated by the thermal decomposition of PA6 at temperatures over 573 K,[7,25] and these voids would be formed as a result.

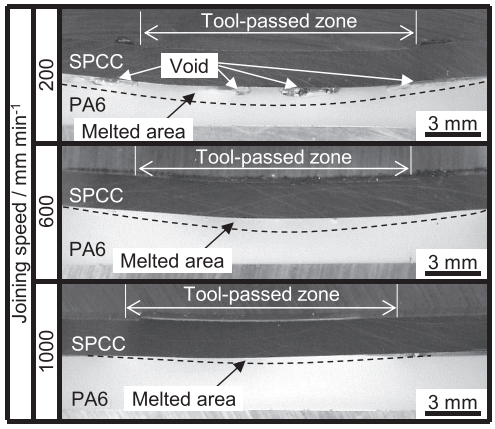

Fig. 7. Cross-sectional macrostructure of FLJ joint of SPCC/PA6 at joining speeds of 200, 600, and 1 000 mm min^{-1}.

Figure 8 shows the relation between the joining speed and the weight-average molecular weight of PA6 near the interface of the FLJ joint and in the as-received PA6, as measured by GPC analysis.

The weight-average molecular weight of PA6 decreased under heating during FLJ; it also decreased with the joining speed. At lower joining speeds, PA6 was subjected to higher temperatures for a longer duration, which promoted the thermal decomposition of PA6.

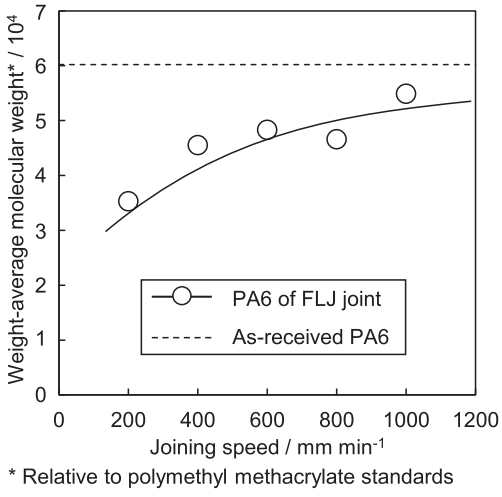

Fig. 8. Relation between the joining speed and the weight-average molecular weight of PA6 of the FLJ joint.

Figure 9 shows the relation between the joining speed and the tensile shear fracture load of FLJ joints of SPCC/PA6 and PE subjected to corona discharge treatment for 5 min. In Fig. 9, the white circles (○) indicate plastic base plate fracture, and the crosses (×) indicate interfacial fracture. The tensile shear fracture load of the FLJ joints of SPCC/PA6 and corona-discharge-treated PE increased with the joining speed up to 600 mm min^{-1}, beyond which it decreased. The tensile shear fracture load of SPCC/PA6 and corona-discharge-treated PE joints fabricated at 600 mm min^{-1} were 1.72 and 0.95 kN, on average. **Figure 10** shows the appearance of fractured joints of (a) SPCC/PA6 and (b) corona-discharge-treated PE after the tensile shear test. The presence of bulk PA6 and PE was determined on

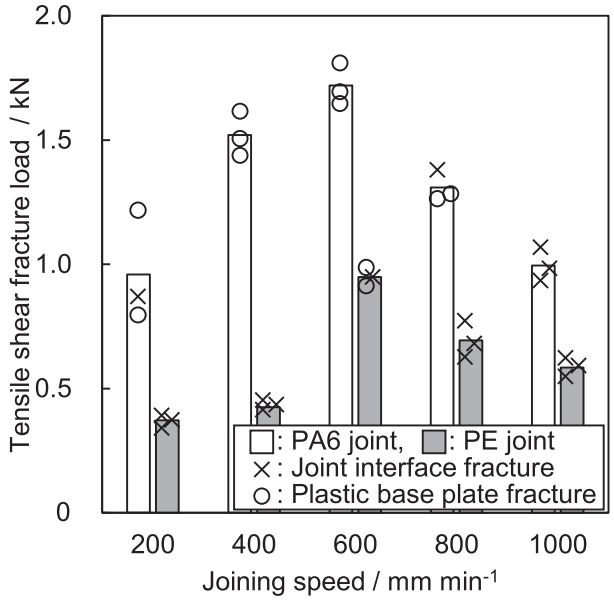

Fig. 9. Relation between the joining speed and the tensile shear fracture loads of FLJ joints of SPCC/PA6 and corona-discharge-treated PE.

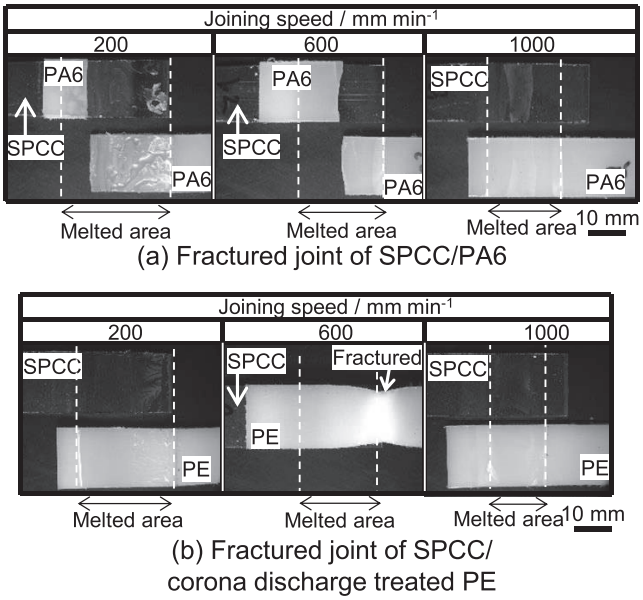

Fig. 10. Appearance of fractured joints of (a) SPCC/PA6 and (b) corona-discharge-treated PE after tensile shear test.

the SPCC side of the fractured joint surface prepared at a joining speed of 600 mm min^{-1}, which indicates that the PA6 and PE matrix fractured. At joining speeds higher than 600 mm min^{-1}, the PA6 and PE joints fractured at the joint interface. Thin residual PA6 and PE were observed on the SPCC side even with the interface fracture. At lower joining speeds, voids were observed in the residual PA6 and PE on the SPCC side. At these joining speeds, the main fractured positions of the PA6 joints were at the PA6 base plate, whereas those of PE were at the interface of the joint. The melted area of PA6 and PE corresponding to the joined area, which was measured by the fractured surface, increased with decreasing joining speed.

4. Discussion

With regard to the effect of polar groups on joining properties, PA6 and corona-discharge-treated PE could be joined to SPCC, whereas as-received PE could not. Direct joining of metal/plastic was accomplished by the bonding between the plastic surface and the surface oxide layer of the metal. Various joining mechanisms such as chemical bonding (covalent bonding, hydrogen bonding), Van der Waals force, and the anchor effect have been reported to provide the bonding force for these materials.[9,26,27] The hydrogen bonding between the metal oxide (or hydroxide) layer on a metal surface and (1) a polar group, such as the hydroxyl (-OH) or carboxyl (-COOH) group, in corona-discharge-treated PE, and (2) the amide group (CONH) in PA6, has often been attributed with providing an effective joining force for direct joining of these materials.[9,21–24,26] The polar group in plastic materials consists of some atoms that have different electronegativities. For example, the electronegativities of O and H in the hydroxyl (-OH) group are 3.5 and 2.1, respectively.[28] O and H in this polar group are polarized as O ($-\delta$) and H ($+\delta$) owing to the difference in electronegativities. Moreover, metal oxides are also polarized. In this study, Fe_3O_4 was detected as the metal oxide at the interface of SPCC/PA6, as shown by TEM analysis (Fig. 3). The electronegativity of Fe is 1.8, and that of O is 3.5; thus, Fe_3O_4 was polarized as Fe ($+\delta$) and O ($-\delta$).[21–23,26] Therefore, these materials were joined by Coulomb's force (hydrogen bonding) between Fe_3O_4 and the polar group in the plastic. The amide (-CONH-) group of PA6 and the carboxyl (-COOH) group of corona-discharge-treated PE, which were detected by XPS analysis (Fig. 2), were also polarized owing to the difference in electronegativities. These polar groups facilitate the direct joining of SPCC to PA6 and corona-discharge-treated PE. As-received PE is non-polar; hence, it cannot be joined to SPCC.

As in previous studies, dissimilar joint formation of Mg and Al alloys with plastic by FLJ was investigated.[20,21] MgO for Mg alloy/plastic, and MgO and Al_2O_3 for Al alloy/plastic were observed as oxide layers of these metals at these interfaces. It was indicated that these materials were also joined because of the Coulomb's force (hydrogen bonding) between the oxide layers of the metals and the polar group of plastics as well as plain carbon steel/plastic, as shown in Fig. 3. As the electronegativities of Mg and Al are 1.2 and 1.5,[28] respectively, the Coulomb's force between Mg oxide and Al oxide to plastics, which arose by the polarization of metal oxides and plastics, would be higher than that of Fe_3O_4 of steel to plastic. Therefore, it is considered that the joining strength of Mg alloys and Al alloys to plastics would also be higher than that of steel to plastic. However, the joints of Mg alloy/, Al alloy/, and SPCC/plastic were fractured at the plastic base materials under the suitable joining conditions as well as under considerably different joining conditions between SPCC and lightweight metals. Thus, it was difficult to compare these joining strengths.

With regard to the effect of joining speed, the tensile shear fracture load decreased as the joining speed increased from 600 to 1 000 mm min^{-1}, and fracture mainly occurred at the interface of SPCC/plastic at higher joining speeds because of the insufficient heat input. The temperature was

too low and the melting duration was too short; thus, the wetting of molten plastic on SPCC was insufficient. The joined area increased with decreasing joining speed, as shown in Fig. 10. In contrast, the tensile shear fracture load of the SPCC/PA6 and PE joints decreased with the joining speed below 600 mm min^{-1}. This can be attributed to the void formation and thermal decomposition of the plastics, as shown in Fig. 8.

5. Conclusions

Direct joining of polyamide 6 and polyethylene plates to a plain carbon steel (SPCC) plate was performed using friction lap joining (FLJ). The polar groups on the plastic surface and the joining speed were investigated in terms of their effect on the FLJ joint characteristics. The following conclusions were drawn.

(1) Polyamide 6 and SPCC plates could directly be joined by FLJ, whereas polyethylene and SPCC plates could not. Corona discharge treatment of the polyethylene surface facilitated joint formation with SPCC. The FLJ joints of SPCC/PA6 and SPCC/corona-discharge-treated PE were fractured at the base materials of the plastic plates under the optimal joining condition in the tensile shear test.

(2) A continuously joined interface of SPCC/plastic was obtained. Voids were formed at the interface in the plastic at low joining speeds. These materials were joined through the oxide layer of SPCC, composed of Fe_3O_4.

(3) The tensile shear fracture load increased with the joining speed up to 600 mm min^{-1}, beyond which it decreased. The joined area increased as the joining speed decreased; however, the joint strength decreased owing to thermal decomposition of the plastic at lower joining speeds.

Acknowledgements

This work was partly supported by a future pioneering project commissioned by the New Energy and Industrial Technology Development Organization (NEDO), and JSPS KAKENHI Grant Number 26820326.

REFERENCES

1) K. Ohishi and H. Fujii: *Materia Jpn.*, **53** (2014), 603.
2) C. Soutis: *Mater. Sci. Eng. A*, **412** (2005), 171.
3) S. Y. Fu, B. Lauke, E. Mäder, C. Y. Yue and X. Hu: *Compos. Part A*, **31** (2000), 1117.
4) F. Razaei, R. Yunus and N. A. Ibrahim: *Mater. Des.*, **30** (2009), 260.
5) V. K. Stokes: *Polym. Eng. Sci.*, **29** (1989), 1310.
6) B. S. Kumar, I. Sridhar, S. Sivashanker, S. O. Osiyemi and A. Bag: *Mater. Sci. Eng. B*, **132** (2006), 113.
7) X. Tan, J. Zhang, J. Shan, S. Yang and J. Ren: *Compos. Part B*, **70** (2015), 35.
8) S. Katayama and Y. Kawahito: *Scr. Mater.*, **59** (2008), 1247.
9) M. Hino, Y. Mitooka, K. Murakami, K. Urakami, H. Nagase and T. Kanadani: *Mater. Trans.*, **52** (2011), 1041.
10) F. Balle, G. Wagner and D. Eifler: *Adv. Eng. Mater.*, **11** (2009), 35.
11) P. Mitschang, R. Velthuis, S. Emrich and M. Kopanarski: *J. Thermoplast. Compos. Mater.*, **22** (2009), 767.
12) S. T. Amancio-Filho, C. Bueno, J. F. dos Santos, N. Huber and E. Hage: *Mater. Sci. Eng. A*, **528** (2011), 3841.
13) F. Yusof, Y. Miyashita, N. Seo, Y. Mutoh and R. Moshwan: *Sci. Technol. Weld. Joi.*, **17** (2012), 544.
14) T. Ozawa, K. Katoh and M. Maeda: *J. Jpn. Inst. Light Met.*, **65** (2015), 403.
15) W. Ratanathavorn and A. Melander: *Sci. Technol. Weld. Join.*, **20** (2015), 222.
16) D. Kitagawa, K. Nagatsuka and K. Nakata: Proc. of the 1st Int. Joint Symp. on Joining and Welding, Woodhead Publishing Ltd., Cambridge, (2013), 111.
17) T. Okada, S. Uchida and K. Nakata: *Mater. Sci. Forum*, **794–796** (2014), 395.
18) F. C. Liu, J. Liao and K. Nakata: *Mater. Des.*, **54** (2014), 236.
19) F. C. Liu, K. Nakata, J. Liao, S. Hirota and H. Fukui: *Sci. Technol. Weld. Join.*, **19** (2014), 578.
20) F. C. Liu, J. Liao, Y. Gao and K. Nakata: *Sci. Technol. Weld. Join.*, **20** (2015), 291.
21) K. Nagatsuka, T. Onoda, T. Okada and K. Nakata: *Q. J. Jpn. Weld. Soc.*, **32** (2014), 235 (in Japanese).
22) K. Nagatsuka, S. Yoshida, A. Tsuchiya and K. Nakata: *Compos. Part B*, **73** (2015), 82.
23) K. Nagatsuka, B. Xiao, A. Tsuchiya, M. Tsukamoto and K. Nakata: *Trans. JWRI*, **44** (2015), 9.
24) K. Nagatsuka, H. Tanaka, B. Xiao, A. Tsuchiya and K. Nakata: *Q. J. Jpn. Weld. Soc.*, **33** (2015), 317 (in Japanese).
25) S. Straus and L. A. Wall: *J. Res. Nat. Bur. Stand.*, **60** (1958), 39.
26) T. Ogawa: Secchaku-Handbook, 4th ed., Nikkan Kogyo Shimbun, Ltd., Tokyo, (2007), (in Japanese).
27) W. P. Vellinga, G. Eising, F. M. de Wit, J. M. C. Mol, H. Terryn, J. H. W. de Wit and J. T. M. D. Hosson: *Mater. Sci. Eng. A*, **527** (2010), 5637.
28) Metals data book, 3rd ed., Maruzen, ed. by the Japan Institute of Metals, Tokyo, (1995), (in Japanese).